doi.org/10.36721/PJPS/2026.40.16509.1

Oleanolic acid nanoparticle-integrated gel: A novel topical approach for antimicrobial therapy

Amna Naz[1], Rouheena Shakir[2], Sadia Haider[2], Nadia Anwar[2], Sana Saeed[1], Rabia Khokhar[3], Habiba Rafique[2], Haider Ali[2], Huzaifa Rana[2], Hafiz Arfat Idrees[4], Sheryar Afzal[5] and Muhammad Farooq[6*]

[1]Gulab Devi Institute of Pharmacy, Lahore, Pakistan
[2]Leads College of Pharmacy, Lahore Leads University, Lahore, Pakistan
[3]Institute of Pharmaceutical Sciences, University of Veterinary and Animal Sciences, Lahore, Pakistan
[4]Faculty of Pharmacy and Biomedical Sciences, MAHSA University, Malaysia
[5]Department of Biomedical Sciences, College of Veterinary Medicine, King Faisal University, Al-Ahsa, Saudi Arabia
[6]School of Pharmacy, Multan University of Science and Technology, Multan 59201, Pakistan

Abstract: **Background**:Topical oleanolic acid (OA) delivery is challenged by poor aqueous solubility and limited skin permeation, necessitating nanoparticle-based and bioadhesive gel systems to improve dermal retention. **Objectives**: This study aimed to develop and evaluate a topical gel formulation incorporating oleanolic acid nanoparticles (OANPs) to enhance the solubility and therapeutic efficacy of OA. **Methods**: OANPs were formulated using the nanoprecipitation technique and assessed for various physicochemical tests, whereas comprehensive gel assessment included physical appearance, pH, viscosity, spreadability *and in-vitro* drug release. In addition, scanning electron microscopy (SEM) analysis and an *in-vivo* skin irritation test were also conducted. A comparative analysis of *ex-vivo* drug permeation was also accomplished for free OA suspension, OANPs (F3) and OAG1. **Results**: The optimized OANPs (F3) maintained a mean nanoparticle size of 12.81 nm, making it more suitable for dermal application. Values of % entrapment efficiency (E.E), polydispersity index (PDI) and zeta potential were 79.18%, 0.32 ± 0.04 *and* -26.2 ± 1.2 mV, respectively, thus displaying maximum % EE, uniform size distribution *and* good colloidal stability. OANPs (F3) showed strong free-radical scavenging potential. Likewise, antimicrobial testing revealed notable zones of inhibition (ZOI) against *Escherichia coli*, *Pseudomonas aeruginosa* and *Staphylococcus aureus*, confirming the effective bioactive potential. Oleanolic acid nanoparticle integrated gel formulation1(OAG1) demonstrated desirable *ex-vivo* drug release and permeation up to 36 h, along with no signs of irritation, redness, or lesions upon *in-vivo* skin irritation testing. **Conclusion**: OANPs were optimized, and the selected formulation (F3) was incorporated into a bioadhesive gel (OAG1) to overcome the poor aqueous solubility and limited skin permeation of OA. Both F3 and OAG1 showed comparable *ex vivo* drug release and permeation; however, OAG1 significantly improved OA skin retention due to its optimized viscosity, polymeric composition, improved antimicrobial action and bioadhesive properties.

Keywords: Antibacterial; Antioxidant; *Ex-vivo permeation*; *In-vivo* skin irritation; Nanogel; OANP

Submitted 27-03-2026 – Revised 29-07-2026 – Accepted 29-07-2026

INTRODUCTION

Oleanolic acid (OA) is a naturally occurring pentacyclic triterpenoid found in various plants, including olives and medicinal herbs (Jiang *et al*., 2016). With the molecular formula $C_{30}H_{48}O_3$ and a molecular weight of 456.70 g/mol (Castellano *et al*., 2022), OA exhibits diverse pharmacological properties, such as anti-inflammatory, antimicrobial, antioxidant, anticancer, antiviral and anti-diabetic effects (Naz *et al*., 2026; Tang *et al*., 2022). Despite having multiple therapeutic actions, its applicability in clinical settings is limited as it belongs to biopharmaceutical classification (BCS) class IV, exhibiting low permeability and solubility (Wasim and Bergonzi, 2024). Therefore, its poor bioavailability necessitates the use of advanced drug delivery strategies. Two primary approaches may improve its effectiveness: first, novel dosage forms such as liposomes, nanoparticles (NPs) and phospholipid complexes to enhance absorption and cellular uptake. Secondly, structural modifications to create more bioactive derivatives for improved therapeutic efficacy (Naz *et al*., 2025; De Stefani *et al*., 2022).

Indeed, nanotechnology-based drug delivery systems offer a revolutionary approach to overcoming the limitations of conventional drugs (Xie *et al*., 2016). Besides, NPs provide enhanced stability, controlled drug release, site-specific targeting *and* improved bioavailability (Pirtarighat *et al*., 2019). Thus, NPs effectively penetrate tissues due to their small size (1-100 nm), thereby increasing drug retention and reducing toxicity. Advancements in nanodrug delivery have transformed treatment for various diseases, enabling precise targeting via the enhanced permeability and retention (EPR) effect (Yan *et al*., 2020). This allows the nanoparticles to exhibit the intended pharmacological activity while containing the essential amounts of drugs and releasing drugs to achieve target-specific action (Patil *et al*., 2021). Moreover, the development of NPs through top-down and bottom-up synthesis methods ensures

*Corresponding author: e-mail: farooqali10@yahoo.com

Article in Press

precise control over particle size and surface properties, optimizing drug absorption and cellular uptake. Additionally, nanotechnology has emerged as a promising niche, emphasizing the disruption of the stratum corneum barrier to achieve better permeation in topical drug delivery compared to conventional regimens (Nnamani *et al*., 2021). With further research advancement in nanotechnology, OA-based nanoformulations hold significant promise for future antimicrobial, anticancer, anti-obesity and metabolic disorder treatments (Rahim *et al*., 2021).

A nanogel is a nanosized three-dimensional chain network in which hydrophilic polymers are cross-linked/cross-connected either physically or chemically. They have a tremendous ability to swell by means of holding excess water (Botha *et al*., 2023). This, in turn, provides better occlusivity by preventing trans-epidermal water loss when subjected to topical application (Kesharwani *et al*., 2020). Owing to various attributes such as high drug loading, biocompatibility, stability, biodegradability, maximum surface area, ease of manufacturing, bioadhesion and maximum retention and controlled drug release, nanogels are considered an efficient and promising vehicle for topical drug delivery (Tetik *et al*., 2021). Moreover, nanogels are known for their better penetration and diffusion via protracted drug release and physiologic membranes; therefore, they are considered more stable as sustained drug carriers compared to traditional topical applications such as lotions, creams *and* oils (Sindhu *et al*., 2022a; Sindhu *et al*., 2022b).

Therefore, the current study presented an OANPs-integrated gel formulation to achieve improved, controlled permeation and therapeutic efficacy of OA, thereby avoiding frequent dosing. The study was also evaluated as a novel topical approach for antimicrobial therapy.

MATERIALS AND METHODS

Chemicals

OA, Dimethyl formamide (DMF) and Poloxamer 188 were purchased from Shanghai Aladdin Bio-Chem Technology Co., Ltd., China. Whereas Carbopol (CP), 1,1-diphenyl-2-picrylhydrazyl (DPPH) and triethanolamine (TEA) were procured from J K Enterprises (Pvt.) Ltd. Besides, Glycerin was obtained from Oleocorp (Pvt.) Ltd and propylene glycol (PG) was acquired from AD chemicals. While Hydroxypropyl Methylcellulose (HPMC) was collected from Merck chemicals (Pvt.) Ltd. All chemicals and reagents used in the study were of analytical grade.

Preparation of OANPs

The nanoprecipitation technique was utilized to formulate OANPs. The composition of various formulations is given in table 1, while the schematic diagram is presented in figure (1). Firstly, the organic phase was prepared by dissolving 5 mg of OA in 0.5 mL of DMF. Then, the aqueous phase was prepared by combining 4 mg of Poloxamer 188 with 5 mL of deionized water. Afterward, using a syringe and a magnetic stirrer (Thermo Fisher Scientific) set to 300 rpm, 5 mL of the organic phase containing the drug was added dropwise to the aqueous phase. The resultant mixture was then subjected to magnetic stirring for approximately 30 minutes (mins) to facilitate evaporation of the volatile solvent. Following this, the mixture underwent sonication by using sonicator (Thermo Fisher Scientific) for 10 mins (Alwan and Rajab, 2021).

Characterization of OANPs

Prepared OANPs (F1-F5) were evaluated for further parameters such as Entrapment efficiency (E.E %), viscosity, surface tension, pH, specific gravity and density. Moreover, the optimized formulation (F2) was characterized for further testing, which includes particle size analysis, zeta potential, UV–VIS spectrophotometry and *ex-vivo* drug release. Additionally, antioxidant and antimicrobial testing were conducted.

Entrapment efficiency

To calculate E.E, the prepared OANPs (F1-F5) were centrifuged at high speed (14,000 rpm) for approximately 15 mins by using centrifugation machine (Thermo Fisher Scientific) to separate the OANPs from the unloaded drug in the supernatant. The supernatant was used to determine the amount of drug remaining as free drug using a UV-VIS spectrophotometer (UV Shimadzu, Japan) at 254 nm. The absorbance values were used to calculate the amount of drug from a straight-line equation given as equation 1 (Khan *et al*., 2022a).

$$\text{E. E}(\%, {}^{W}/_{W}) = \frac{\text{Total amount of drug} - \text{Amount of drug in supernatant}}{\text{Total amount of drug}} \times 100 \qquad (1)$$

Viscosity

The viscosity of the OANPs dispersion (F1-F5) was measured using an Ostwald viscometer (SI Analytics) at 25 ± 1°C (Poulten Selfe & Lee Ltd., Essex, UK). The instrument was thoroughly cleaned, dried and securely mounted in a vertical position. It was first filled with distilled water up to mark A and the time taken for the liquid to flow down to mark B was recorded. The process was then repeated by replacing distilled water with the OANPs dispersion and the flow time between points A and B was noted. The viscosity of the OANPs was calculated using the following equation as given as equation 2. Measurements were taken in triplicate and the results were expressed as mean ± SD (Khan *et al*., 2022a).

$$\eta 1 = (d1 * t1 - d2 * t2) * \eta 2 \qquad (2)$$

Where

η 1Viscosity of the OANPs sample
η 2: Viscosity of the pure distilled water
t1: Flow time of pure distilled water
t2: Flow time of OANPs sample
d1: Density of OANPs sample
d2: Density of pure distilled water

Article in Press

Table 1: Composition of OANPs formulations.

Sr. no.	Chemicals	F1	F2	F3	F4	F5
1	OA (mg)	2	2	2	2	2
2	DMF (mL)	0.5	0.5	0.5	0.5	0.5
3	Poloxamer 188 (mg)	2.5	3	4	4.5	5
4	Deionized water (mL)	5	5	5	5	5

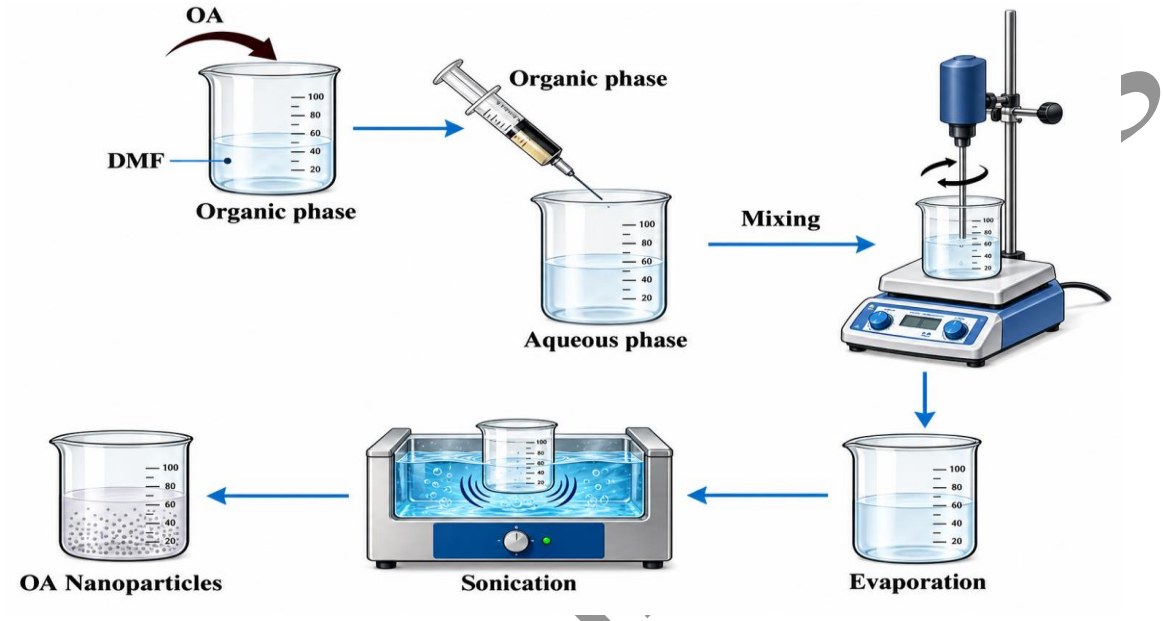


Fig. 1: Schematic illustration of the preparation of oleanolic acid nanoparticles formulations.

Surface tension

The surface tension of the OANPs (F1-F5) was measured using a laboratory stalagmometer (Samtech Instruments). Before use, the stalagmometer was thoroughly cleaned with deionized water and dried. It was then filled with double-distilled water up to point A. The water was allowed to flow drop by drop until it reached point B and the number of drops was recorded. The same procedure was repeated for the OANPs and the density of the OANPs was determined using the equation 3(Khan *et al*., 2022a).

$$\gamma 1 = (\delta 1 * n1 \div \delta 2 * n2) * \gamma 2 \quad (3)$$

Where

$\gamma 1$ = Surface tension of dispersion;
$\gamma 2$ = Surface tension of water;
$\delta 1 = Density\ of\ dispersion$;
$\delta 2$ = Density of water;
n1 = Number of drops of OANPs;
n2 = Number of drops of de-ionized water

Density

The density of the synthesized OANPs (F1-F5) was measured using a pycnometer (DWK Life Sciences) at a temperature of 25 ± 1 ºC. First, the weight of the empty pycnometer with a known volume (V) was recorded as W1. Next, the pycnometer was filled with water and its weight was noted as W2. Then, the pycnometer filled with OANPs was weighed and labeled as W3 (Khan *et al*., 2022a). The following equations 4 and 5 were used to determine the density of the OANPs.

$$Density\ of\ Water = \frac{W2}{V} \quad (4)$$

$$Density\ of\ OANPs = \frac{W3}{V} \quad (5)$$

Specific gravity

After measuring density, the specific gravity of OANPs (F1-F5) was estimated by the equation 6 mentioned below (Khan *et al*., 2022a).

$$Specific\ gravity\ of\ OANPs = \frac{(\text{OANPs density})}{(\text{Water density})} \quad (6)$$

Fourier Transform Infrared

Fourier Transform Infrared (FTIR) spectroscopy (Thermo Fisher Scientific) was carried out to examine the characteristic functional groups of the components and to explore any potential interactions between the drug and the excipients. The analysis included pure OA, poloxamer and the final nanoparticle formulation. For sample preparation, each was carefully mixed with dry potassium bromide (KBr), ground into a fine powder and then compressed into a transparent pellet using a vacuum-assisted hydraulic press. Spectra were recorded over the 4000 to 400 cm^{-1} wavelength range at a resolution of 4 cm^{-1}, averaging 16 scans per sample to ensure accuracy (Shi *et al*., 2021).

Article

In-vitro drug release

Drug release from the OANPs (F1-F5) was evaluated using a Franz diffusion cell (PRIME GEAR Inc., No. 4G 1-22-3-12, India). A cellulose acetate membrane (0.45 µm) was securely placed between the donor and receptor compartments. The receptor compartment was filled with phosphate buffer (pH 7.4) and maintained at 32 ± 2°C to mimic skin conditions. Magnetic stirring was set at 600 rpm to ensure sink conditions. The donor compartment was loaded with 1 g of the sample. At specific intervals, a 0.5 mL aliquot was withdrawn. An equal volume was replenished from the receptor compartment via the sampling port. The mixture was analyzed using a UV-VIS spectrophotometer at a specified wavelength (254 nm). The cumulative release of OANPs from the carrier system was determined using a standard calibration curve. All results were recorded as the mean of three independent experiments (Gulcin and Alwasel, 2023).

Based on the above results, OANPs formulation (F3) with maximum % E.E and *ex-vivo* drug release was selected for further evaluation, such as particle size, zeta potential and biological activities such as antioxidant and antimicrobial potential.

Characterization of OANPs (F3)

Determination of particle size, polydispersity index (PDI) and zeta potential

OANP formulation (F3) was characterized for particle size, polydispersity index (PDI) and zeta potential using a NanoBrook® Zetasizer (Zetasizer Nano). After diluting OANPs (F3) 1:1000 (v/v) with distilled water, the samples were mixed using a magnetic stirrer to inhibit particle aggregation and minimize the degree of proximity. Measurements were performed in triplicate (Gulcin and Alwasel, 2023; Naz *et al*., 2025).

Analysis of Antioxidant activity

The antioxidant potential of OANPs (F3) was assessed by evaluating its ability to reduce the activity of DPPH radicals. Firstly, the formulation (1 mg/mL) was diluted to prepare a 100 µg/mL solution. A 1 mL sample of OANPs F3 (100 µg/mL) was combined with 9 mL of DPPH solution (0.1 mM in methanol). The DPPH solution served as a positive control. The samples were vigorously shaken and incubated in the dark at room temperature for 24 hours. At specified time intervals (1, 2, 4, 8, 12, 24 hours), samples were withdrawn and their absorbance was measured by UV-VIS spectrophotometer. Ascorbic acid was used as the reference material for determining absorbance at 517 nm (Naz *et al*., 2025). The equation 7 was used to estimate the scavenging effect (Khan *et al*., 2022b).

$$Scavenging\ effect(\%) = \frac{\text{Control}-\text{Sample}}{\text{Control}} \times 100 \qquad (7)$$

Analysis of Antimicrobial activity

Formulation F3 of OANPs was evaluated for its antimicrobial potential against highly pathogenic gram-negative (*E. coli* and *P. aeruginosa*) and gram-positive (*S. aureus*) microbes. The Muller-Hinton agar standard and the well diffusion technique were used in a petri dish to test the antimicrobial activity of F3. Bacterial cells were cultured in nutrient broth for 24 hours at 37 °C before being spread out onto Muller-Hinton agar plates in a laminar flow cabinet (Thermo Fisher Scientific). Four wells, each 5 mm in diameter, were then drilled into the agar gel with a sterile loop. A micropipette was used to dispense the required amount of OANPs into each well. Finally, the plates were re-incubated at 37 °C for another day in an incubator (National Incubation Center Lahore). Following the preparation of the bacterial plates, the zone of inhibition of the OANPs was measured after 24 hours of incubation at 37 °C (Khan *et al*., 2022b).

Preparation of OANPs integrated gel formulations

Further, the gel containing OANPs (F3) was synthesized using a dispersion-swelling method with CP and HPMC. The excipients were accurately weighed according to the specified formulation (OAG1-OAG3) as presented in table 2. Afterward, CP and HPMC were dissolved in water and allowed to stand for 4 hours to ensure adequate polymer swelling. Subsequently, OANPs formulation (F3) of 0.5 mg/g was gradually incorporated into the polymer gel with continuous, unidirectional stirring to prevent the formation of air bubbles. Then, TEA was added to facilitate crosslinking between CP and HPMC, thereby forming a stable gel matrix. Then, glycerin and PG were subsequently added to modify the gel's viscosity. Finally, the pH was adjusted to 7.4 ± 0.1 using 0.1 N NaOH (Gulcin and Alwasel, 2023).

Characterization of OANPs integrated gel (OAG1-OAG3)

Physical appearance

For the formulation (OAG1-OAG3), fundamental characteristics were assessed. Each gel (OAG1-OAG3) was assessed for color, transparency, consistency, homogeneity and grittiness; therefore, overall appearance was evaluated through visual inspection (Khan *et al*., 2022b).

pH

The pH of the gel's 0.5% aqueous solution was measured using a pH meter (Accumet meter) at 25 ± 1 ºC. One gram of gel was dissolved in 100 mL of distilled water and allowed to stand for 2 hours before measurement. Thus, pH was tested by placing the pH meter electrode in each gel (OAG1-OAG2). The reading was noted until it stabilized. The experiment was done in triplicate and the mean value was calculated ± SD (Perry and Wren, 2026).

Article in Press

Table 2: Composition of gel formulations for OANPs (OAG1-OAG3).

Sr. no.	Ingredients (%)	OAG1	OAG2	OAG3
1	Carbopol	1.5	1.0	0.5
2	Hydroxypropyl methylcellulose	0.5	1.0	1.5
3	Glycerol	10	10	10
4	Triethanolamine	2	2	2
5	Propylene glycol	5	5	5

Viscosity and spreadability

The viscosity of gel formulations (OAG1-OAG3) was measured by the same procedure as described above. For spreadability, 1g of each gel formulation was placed between two slides, covered with a pre-weighed plate and the weight was increased steadily until the gel stopped spreading to test the gel's spreadability. Both the final weight and the time required for gel diffusion were measured and recorded independently. The equation number 8 was then used to determine the gel's spreadability; that is, the time difference between the mass of the gel and the total weight applied (Alwan and Rajab, 2021).

$$Spreadibility = \frac{\text{Mass} \times \text{Length}}{\text{Time}} \quad (8)$$

In-vitro drug release of OANPs

The OA release from the OANP gels (OAG1-OAG3) was also assessed using a Franz diffusion cell, following the same procedure described above for estimating drug release from OANPs. The experiment was done in triplicate and the mean was taken as the result (Agrawala et al., 2015; Iriventi *et al*., 2020).

Based on the oleanolic acid release profile of formulations OAG1–OAG3, the optimized formulation was selected for SEM analysis. The selection was based mainly on the formulation that exhibited the most desirable and controlled drug-release behavior, without excessive burst release or incomplete release.

Scanning electron microscopy of OAG1

To observe the particle surface and morphology of gel formulation OAG1, SEM (Thermo Fisher Scientific) analysis was conducted. To ensure optimal imaging conditions, the sample preparation procedure was performed meticulously. For stable imaging, the sample was mounted onto SEM stubs using double-sided conductive adhesive tape. A thin layer of gold was then sputter-coated onto the surface to enhance electrical conductivity, minimize charging effects and improve image clarity and resolution during SEM analysis (Farooq *et al*., 2020).

In-vivo skin irritation test

Acute skin irritation that may arise from any formulation component was assessed in human skin. To enhance the efficacy of the study, five human volunteers were selected. On the back of the hand, 1g of gel (OAG1) was applied to an area of two square inches. Afterward, any signs of edema or erythema, redness, or lesions were observed for the next 24, 48 and 72 hours of application (Talele *et al*., 2017).

Ex-vivo drug permeation and retention

The effectiveness of topical and transdermal drug delivery largely depends on the drug's capacity to penetrate the stratum corneum, the skin's outermost keratinized layer and accumulate within the targeted tissues. To assess drug permeation from the developed formulations, Franz diffusion cells (Perme Gear, Inc., Hellertown, PA, USA) were used with excised skin from Sprague Dawley rats, as outlined in recent protocols (Pathak *et al*., 2024). A Franz diffusion setup comprising six cells (each with a diffusion area of 0.654 cm^2 and a 5 mL receptor volume) was used under controlled conditions: stirring at 600 rpm and a maintained temperature of 37 °C. Sprague-Dawley rats (weighing 200 ± 20 g) were humanely euthanized by cervical dislocation. Their fur was completely shaved and full-thickness skin sections were excised following guidelines approved by the Ethical Review Committee of the University of Lahore. The excised skin was thoroughly cleaned with saline to remove residual fat and stored at -20 °C in freezer (Whirlpool) until required (Khan *et al*., 2022a). For the permeation analysis, the thawed rat skin was placed between the donor and receptor compartments of the diffusion cells. The receptor side was filled with phosphate buffer (pH 7.4) to maintain sink conditions. Optimized formulations, including drug-loaded OANPs F3, OAG1 and a free OA suspension, were applied to the donor compartment. The apparatus was kept at 37 ± 2 °C with continuous stirring throughout the experiment. At predetermined intervals (0, 4, 8, 16, 20, 24, 28, 32 and 36 hours), 0.5 mL samples were withdrawn from the receptor chamber and immediately replaced with fresh buffer solution. Drug levels were analyzed using UV-VIS spectrophotometry at 254 nm (Iriventi *et al*., 2020).

Following the permeation test, drug retention within the skin was evaluated by weighing and homogenizing the used skin. Methanol (10 mL) was added and the mixture was incubated at 37 ± 1 °C overnight in a shaking water bath. A lysis reagent (in a 1:20 ratio) was then introduced, followed by 30 minutes of sonication. The solution was subsequently ultracentrifuged at 12,000 rpm for 20 mins at 10 °C. The retained OA concentration was measured using

Article in Press

the previously validated UV-VIS spectrophotometric technique (254 nm) (Jiamphun and Chaiyana, 2023, Iriventi *et al*., 2020).

RESULTS

Characterization of OANPs (F1-F5)

Physicochemical characterization

Results of various physicochemical parameters of OANPs formulations (F1-F5) are displayed in table 3. Thus, the % E.E of various formulations ranged from 65.41 to 79.18%, with F3 showing the highest % E.E (79.18%). It is evident that varying polymer concentrations significantly affected OA drug entrapment. Moreover, the viscosity of all OANPs (F1-F5) was observed in the range of 9.23 to 32.51, exhibiting a moderately viscous nature.

FTIR

To evaluate potential interactions and confirm successful formulation, the FTIR spectra of OA (A), poloxamer (B) and the final nanoparticle formulation OANPs F3 (C) were carefully analyzed as shown in figure 2. The spectrum of pure OA showed a broad absorption band at approximately 3430 cm^{-1}, characteristic of O–H stretching vibrations. Additional peaks at approximately 2920 cm^{-1} and 2850 cm^{-1} were linked to the C–H stretching of aliphatic chains. A prominent peak near 1705 cm^{-1} indicated the presence of C=O stretching from the carboxylic acid group. Bands between 1450 and 1375 cm^{-1} were associated with bending vibrations of methyl and methylene groups, while those around 1100–1000 cm^{-1} corresponded to C–O stretching, suggesting the presence of both hydroxyl and carboxyl functionalities. In the FTIR spectrum of poloxamer, a broad peak at around 3450 cm^{-1} was observed, corresponding to O–H stretching typically found in polyether compounds. Peaks between 2880 and 2940 cm^{-1} were attributed to symmetric and asymmetric C–H stretching of $–CH_2$ groups. A distinct band near 1100 cm^{-1} confirmed the C–O–C stretching vibrations, characteristic of the poly(ethylene oxide) and poly(propylene oxide) blocks in the polymer.

In-vitro drug release

The *in-vitro* drug release study serves as a crucial predictor of the drug's *in-vivo* performance, offering insight into how the formulation might behave upon administration. So, the percentage drug release from different OANPs formulations (F1-F5) is shown in figure 3a. Based on the above outcomes, the OANPs F3 formulation was found to have maximum EE (79.18%) and *in-vitro* drug release up to 70%. Hence, F3 was further evaluated for particle size, zeta potential, antioxidant and antimicrobial activity. Based on the above outcomes, OANPs F3 formulation was found to have maximum E.E (79.18%) and *in-vitro* drug release up to 70%. Hence, F3 was further evaluated for particle size, zeta potential, antioxidant and antimicrobial activity.

Characterization of OANP (F3)

Particle size, polydispersity index (PDI) and zeta potential

The particle size analysis of the OANPs (F3) revealed one distinct peak as shown in figure 4a. The peak was observed at 12.81 nm. The PDI value was 0.32 ± 0.04, indicating an appreciable size distribution throughout the system and the zeta potential was found to be -26.2 ± 1.2 mV.

Antioxidant potential

The antioxidant potential of ascorbic acid, free OA and OANPs was assessed using the DPPH radical scavenging assay. The DPPH radical-scavenging percentage was measured to assess each sample's ability to neutralize free radicals. As expected, ascorbic acid, the reference antioxidant, exhibited the highest scavenging capacity, with 94.2 ± 1.3% inhibition at the maximum tested concentration. Meanwhile, the DPPH control, which lacked an antioxidant compound, showed minimal inhibition, validating the accuracy of the assay. Free OA exhibited moderate antioxidant activity, with a peak inhibition of 48.5 ± 2.1%, consistent with its known pharmacological profile. Whereas OANPs (F3) displayed 71.6 ± 1.8% inhibition, as shown in figure 4b.

Antimicrobial action

Using the well diffusion method, the antibacterial activity of OANP (F3) was assessed against Gram-negative (*E. coli* and *P. aeruginosa*) and Gram-positive (*S. aureus*) bacteria after 1 day. Thus, values of zones of inhibition (ZOI) for the formulation F3 against different microbes at a concentration of 1 mg/mL are presented in table 4. The outcomes revealed that OANPs (F3) showed significant antimicrobial activity against *Pseudomonas aeruginosa*, with a ZOI of 21 mm, whereas it exhibited good antimicrobial potential against *E. coli* and *Staphylococcus aureus*, with ZOIs of 17 mm and 15 mm, respectively.

Characterization of OANPs integrated gel formulations

Physical appearance

Visual examination revealed that the prepared gels (OAG1-OAG3) were clear and homogeneous, with no sign of grittiness or agglomeration. Apparently, they were white in color. Moreover, the gels did not separate and break whether kept at room temperature or at high temperatures.

pH

For gel formulations (OAG1-OAG3), pH ranged from 7.2-7.4 (table 5). This pH can conveniently be tolerated on skin without any redness, irritation and stimulation (Nikam *et al.*, 2024).

Viscosity and spreadability

Results for OANPs-loaded gel (OAG1-OAG3) characterization are provided in table 5.

Article in Press

Table 3: Outcomes of physicochemical characterization of OANPs (F1-F5) (Mean±SD).

OANPs	% E.E	Viscosity	Surface tension (Dynes/ cm2)	pH	Density	Specific gravity
F1	68.31 ± 2.86	9.23 ± 1.11	25.11 ± 0.26	7.1 ± 2.1	0.981 ± 0.22	0.921 ± 0.32
F2	70.93 ± 1.28	11.46 ± 0.21	23.81 ± 0.34	7.3 ± 1.7	0.932 ± 0.01	0.943 ± 0.13
F3	79.18 ± 2.21	23.62 ± 0.13	20.44 ± 0.78	7.4 ± 1.3	0.998 ± 0.02	0.984 ± 0.04
F4	65.41 ± 1.31	29.82 ± 0.16	19.45 ± 0.55	7.2 ± 1.1	0.945 ± 0.05	0.921 ± 0.04
F5	66.16 ± 0.61	32.51 ± 0.21	18.93 ± 1.28	7.2 ± 1.4	0.932 ± 0.03	0.921 ± 0.03

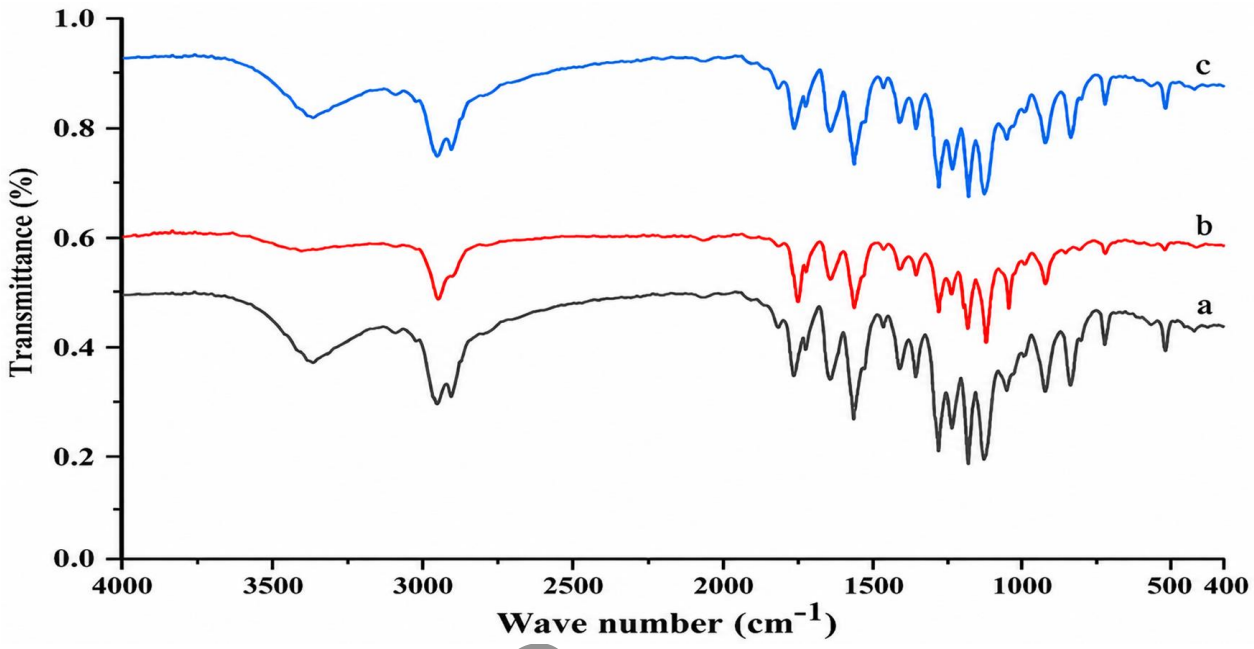


Fig. 2: FTIR spectra of (A) pure oleanolic acid, (B) Poloxamer and (C) oleanolic acid-loaded nanoparticles (F3). The spectra were compared to identify characteristic functional-group absorption bands and to assess possible interactions between oleanolic acid and the excipient after nanoparticle formulation. FTIR, Fourier-transform infrared spectroscopy; F3, optimized oleanolic acid nanoparticle formulation.

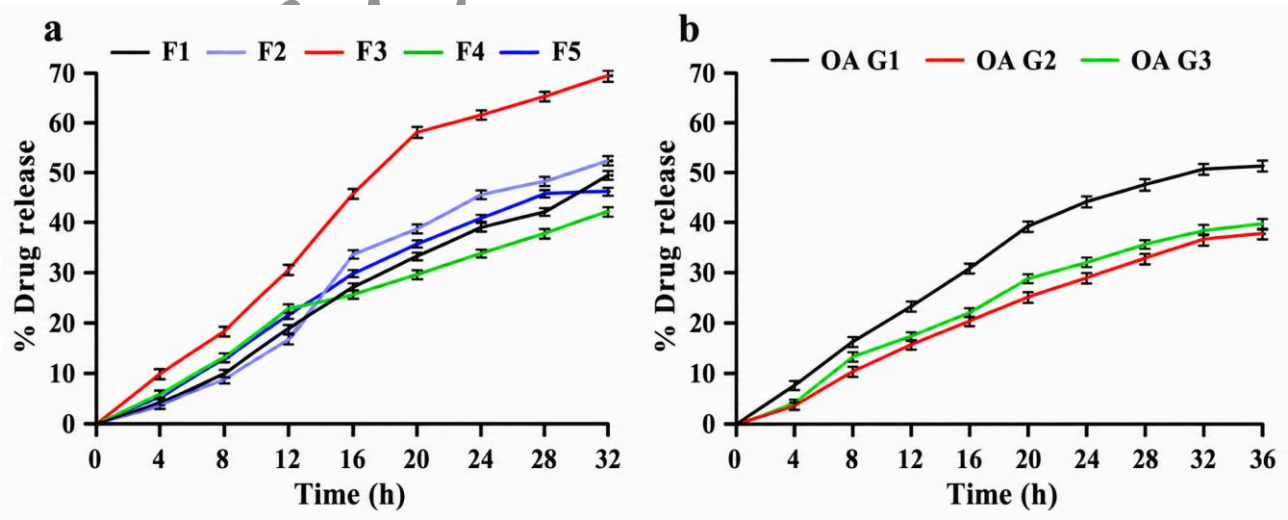


Fig. 3: Drug release. (a) *Ex vivo* drug release (%) of Oleanolic acid from OANPs formulations (F1-F5); (b) *In vitro* drug release (%) of Oleanolic acid from OANPs integrated gel formulations (OAG1-OAG3).

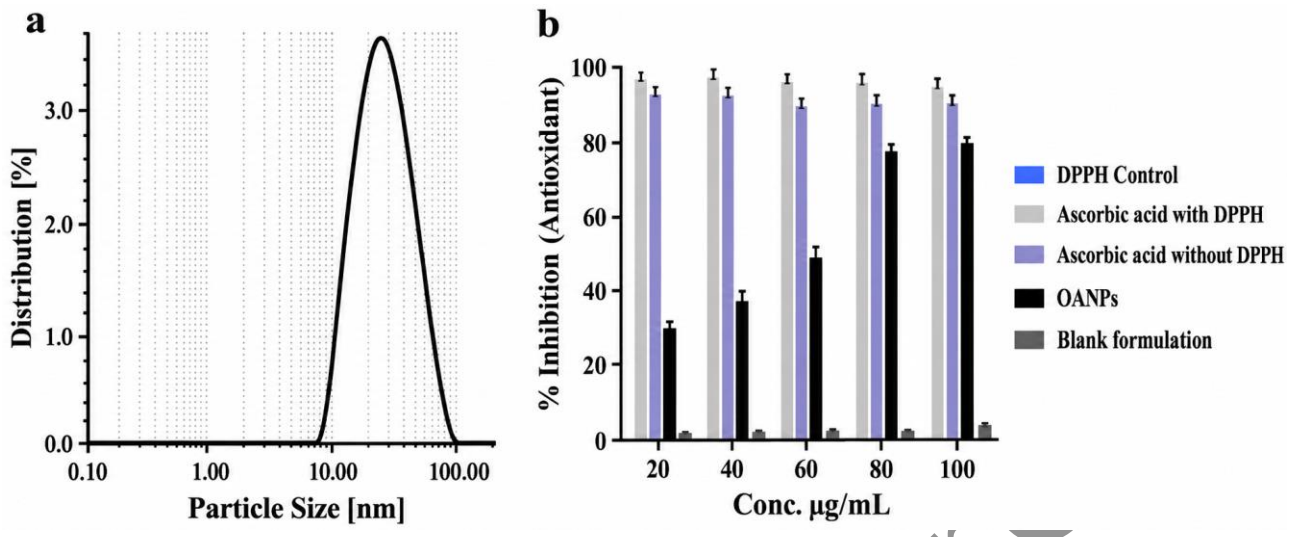


Fig. 4: Characterization and antioxidant activity of oleanolic acid nanoparticles. (a) Particle size distribution of the optimized oleanolic acid nanoparticle formulation (OANPs; F3); (b) Antioxidant activity of OANPs (F3). OANPs, oleanolic acid nanoparticles; F3, optimized nanoparticle formulation.

Table 4: Antimicrobial activity of OANPs (F3) with its respective zones of inhibition (ZOI).

Sr. no.	Test organism	Diameter of zone of inhibition
1	*E.coli*	17 mm
2	*Staphylococcus aureus*	15 mm
3	*Pseudomonas aeruginosa*	21 mm

Outcomes revealed that OANPs (F3) showed significant antimicrobial activity against Pseudomonas aeruginosa, with a ZOI of 21 mm, whereas they exhibited good antimicrobial potential against E. coli and Staphylococcus aureus, with ZOIs of 17 mm and 15 mm, respectively.

Table 5: Viscosity and spreadability of the OANPs loaded Gel.

Sr. no.	Gel formulations	pH	Viscosity (cps)	Spreadability ($g \cdot cm \cdot sec^{-1}$)
1	OAG1	7.3 ± 0.1	17,137 ± 0.12	7.0 ± 0.1
2	OAG2	7.2 ± 0.1	15,295 ± 0.15	6.5 ± 0.2
3	OAG3	7.4 ± 0.1	13,594 ± 0.21	6.3 ± 0.2

In-vitro drug release

The *in-vitro* drug release study serves as a crucial predictor of the drug's *in-vivo* performance, offering insight into how the formulation might behave upon administration. The release of OA from the OANPs gel was found to be highest from OAG1 (> 50%). While the release of OA from the OAG2 and OAG3 was less than 40%.

Scanning electron microscopy

SEM was conducted on the optimized gel formulation OAG1 and the image was shown in figure 5. Micrographs revealed that OAG1 contained spherical nanoparticles with smooth surfaces.

In-vivo skin irritation test

At the end of the study (72 hours), no sign of lesion, irritation, redness, or edema was seen post-application of OAG1 over the skin of human volunteers (Talele *et al*., 2017).

Ex-vivo drug permeation and retention

The permeation profile of OA through the stratum corneum of Sprague Dawley rats, following application of OANPs (F3), OANPs integrated gel (OAG1) and free OA suspension, is presented in figure 6a followed by the retention estimation as shown in figure 6b.

DISCUSSION

Results of physical parameters studies (Table 3) revealed that varying concentrations of polymer significantly altered the drug entrapment of OA. Previously, it was observed that viscosity is a function of surfactant and aqueous phase in a formulation.

Article in Press

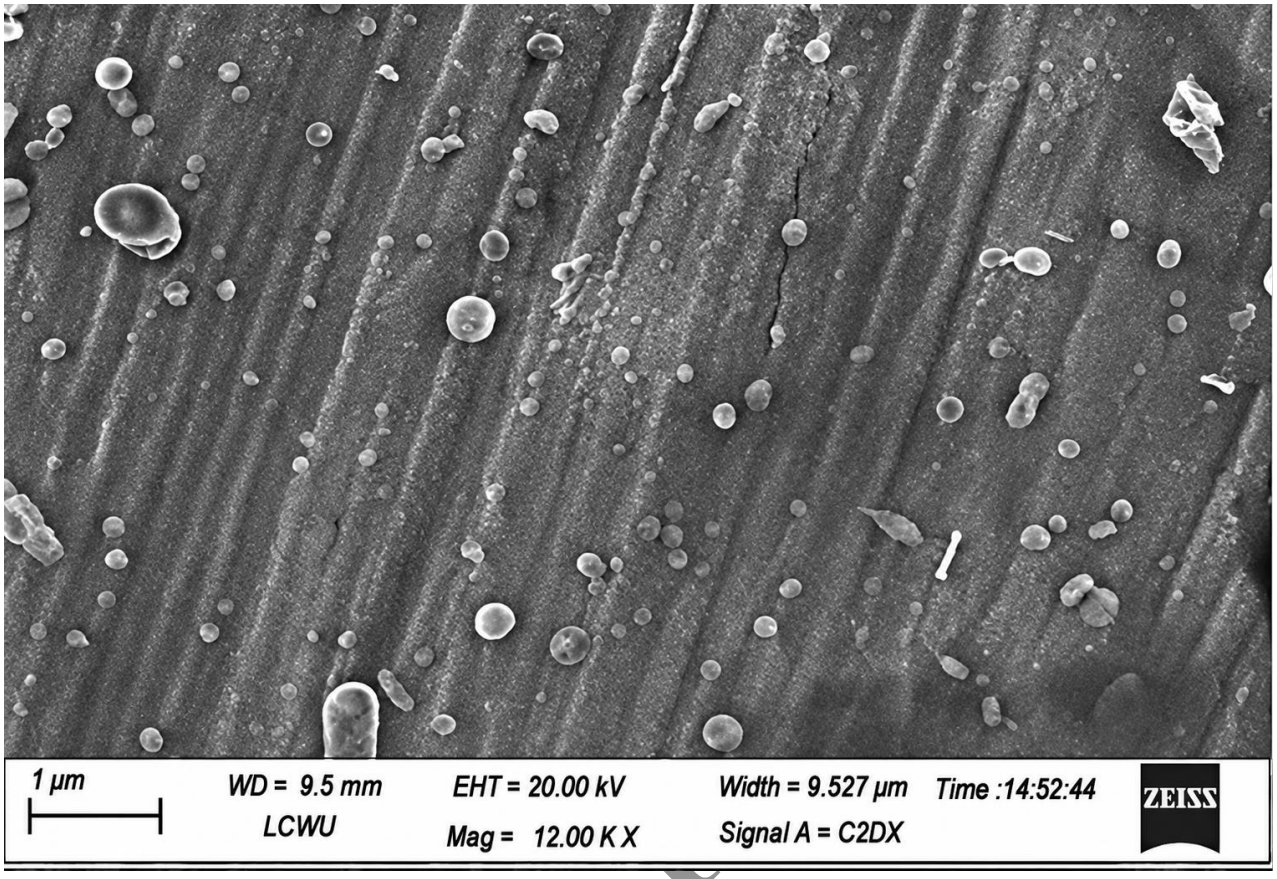


Fig. 5: Scanning electron microscopy (SEM) image of the optimized oleanolic acid nanoparticle integrated gel formulation (OAG1), showing the surface morphology and structural characteristics of the formulation. OAG1: optimized oleanolic acid nanoparticle gel formulation.

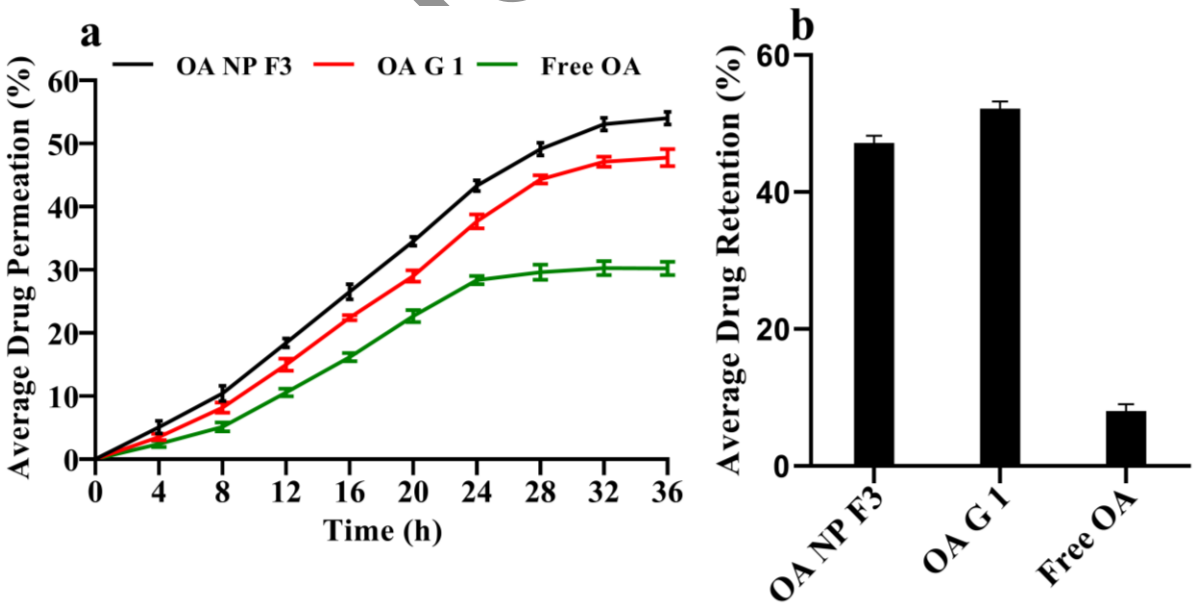


Fig. 6: Drug permeation and retention. (a) *Ex vivo* drug permeation (%) of of oleanolic acid from oleanolic acid nanoparticles (OANPs; F3), oleanolic acid nanoparticle integrated gel (OAG1) and Free OA suspension; (b) Average drug Retention (%) of Oleanolic acid from OANPs (F3), OAG1 and Free OA suspension.

Therefore, increasing the surfactant concentration increased the viscosity of OANPs (F1-F5), which in turn may favor contact of the formulation with the skin and drug release. The relationship between immiscible phases is depicted by surface tension. Surface tension was minimized with increasing surfactant concentration, as seen from F1 to F5. A high level of surfactant reduces surface tension by minimizing the surface area of individual particles. Besides, the pH of all formulations was observed to be within the acceptable range, whereas the results of density and specific gravity were found to be close to those of deionized water. The FTIR profile of the nanoparticle formulation OANPs (F3) revealed significant changes that support successful drug loading. The O–H stretching band appeared broader and slightly shifted to 3420 cm^{-1}, suggesting hydrogen bonding interactions between oleanolic acid and poloxamer. The intensity and position of the C=O stretching peak around 1705 cm^{-1} were reduced and shifted, likely due to partial encapsulation or molecular interactions within the polymer matrix.

While the C–H stretching bands were still visible, their intensity had decreased, which could be attributed to the surface coverage by the polymer in the nanoparticulate form. Additionally, the C–O stretching band near 1100 cm^{-1} appeared less distinct, reinforcing the idea that molecular interactions had occurred during formulation. The most important change was observed in the carbonyl C=O stretching region of oleanolic acid, where the characteristic peak around 1700–1710 cm^{-1} appeared with reduced intensity/slight shifting in the nanoparticle formulation, indicating possible interaction or encapsulation of oleanolic acid within the polymer matrix. In addition, the broad O–H stretching band shifted/broadened around 3400–3420 cm^{-1}, suggesting hydrogen bonding between the hydroxyl group of oleanolic acid and the ether oxygen groups of poloxamer (Mahmood *et al*., 2024).

The release profile of nanoparticle formulations F1-F5 (Fig. 3a) showed that, overall, the drug release from F1 to F5 displayed an initial burst release, followed by a sustained pattern, thereby depicting controlled release behavior. At first, the burst release pattern of all formulations is attributed to OA availability at the interface or in the hydrophilic phase (Mahmood *et al*., 2024). Among different formulations (F1-F3), F3 exhibited the highest drug release, up to 70% at the end of 32 h. This may be attributed to the highest % E.E. (79.18%) coupled with high viscosity and an increased amount of surfactant. However, F4 and F5 displayed OA release up to 38% and 42%, respectively, at the end of the study. This disparity is likely due to the comparatively low % E.E and higher viscosities of F4 and F5, which could have hindered the diffusion of the OA from OANPs.

The particle size of OANPs (F3) was found to be 12.81 nm (Fig. 4a). Values of the peak fall within the normally accepted range of 1 to 100 µm for nanoparticle size, indicating that the OANPs (F3) formulation was appropriately sized for potential biomedical applications. Previous studies have reported that particle sizes below 300 nm are considered favorable for skin uptake, further supporting the suitability of the developed formulation for topical application (Nnamani *et al*., 2021). Whereas, zeta potential (-26.2 ± 1.2 mV) shows that the prepared OANPs (F3) were significantly stable thermodynamically and physically as well, which further favors the storage stability of the prepared formulation. Furthermore, the pronounced value of zeta potential ensured that the prepared OANPs are less prone to coalesce, sediment and aggregate (Pathak *et al*., 2024). The inclusion of carboxylic acid, hydroxyl and methyl groups in OA may be the reason for the partial negative zeta potential that was observed.

Notably, the antioxidant performance improved significantly when OA was delivered in nanoparticle form. The OANPs formulation (F3) achieved 71.6 ± 1.8% inhibition, indicating a substantial enhancement in free radical scavenging compared to the unformulated OA. This observed improvement can likely be attributed to the enhanced solubility, stability and dispersion of OA within the nanoparticle system, which may have facilitated better interaction with DPPH radicals and, consequently, more effective antioxidant action, as shown in figure 4b (Jiamphun and Chaiyana, 2023). Additionally, OANPs (F3) also expressed notable antimicrobial activity against gram-negative (*E. coli* and *P. aeruginosa*) and gram-positive (*S. aureus*) bacteria, thus making it reliable for antimicrobial therapy.

Likewise, characterization of OANPs (F3) integrated gel formulations (OAG1-OAG3) was conducted. It was observed that the viscosity of OANPs was remarkably increased (Table 5) when integrated into gel formulation. Furthermore, gel thickness was more related to the amount of CP rather than HPMC, as HPMC is known for forming a viscous gel. Therefore, an increase in viscosity was seen with the incremental increase in CP concentrations from OAG1 to OAG3. Thus, CP-related thickness was mainly because it binds the solvent in its polymeric structure and yields strong cross-linking with trapped water inside, which further holds the solvent firmly to appear as a rigid gel, more viscous and resistant to pressure and forces (Flieger *et al*., 2021). So, viscosity was found to depend on the polymeric concentration of CP, as it is reported to have concentration-dependent viscosity (Safitri *et al*., 2021).

Nevertheless, spreadability was inversely affected by gel viscosity. Therefore, the spreading power decreased with increasing thickness from OAG1 to OAG3. Despite the variability, all formulations showed easy spreadability upon application to the skin.

Article in Press

In-vitro OA release study of gel formulations (OAG1-OAG3) was performed using Franz diffusion cell and graphical representation is given in figure 3b. Interestingly, when OANPs (F3) were incorporated into a gel base, OA release significantly decreased compared to standalone OANPs. This reduction can be associated with the amount of polymeric blend that imparted remarkable gel viscosity, thus potentially slowing the drug diffusion rate. Among various gel formulations, OAG1 demonstrated the highest drug release, with 50% OA release at the end of 36 h, as shown in figure 3b. Drug release occurred either by diffusion or erosion of the gel matrix (Safitri *et al*., 2021). Moreover, the prolonged release may be due to its optimal viscosity contributed by the polymeric concentration of CP, which allowed better skin adherence and prolonged retention, thus facilitating a more efficient sustained release (Ellakwa *et al*., 2024). Additionally, the presence of HPMC further retarded the diffusion rate. However, OAG2 and OAG3 could release OA up to 40% at the end of the study. This could be attributed to the comparatively low viscosity of OAG2 and OAG3 due to less efficient crosslinking of CP with HPMC. This ultimately decreased gel strength and OA release from gel matrices. Owing to have maximum OA release, OAG1 was selected for further SEM analysis.

Additionally, the SEM image of OAG1 exhibited the presence of spherical nanoparticles (Fig. 5). Besides, the appearance of slightly white scales on the surface may be the result of solvent diffusion (Abu-Rumman *et al*., 2022). Due to the presence of nanoparticles, the gel formulation may effortlessly diffuse and permeate deep in the skin upon topical application. Skin irritation test on human volunteers further suggested the safe application of prepared nanogel formulation (OAG1), as no sign of irritation, lesion, erythema or edema was found.

The *ex-vivo* permeation and retention profile of OA through the stratum corneum of Sprague-Dawley rats, following application of OANP (F3), OANPs integrated gel (OAG1) and free OA suspension, is presented in figures 6a and 6b, respectively. Thus, formulation OANP (F3) emerged with maximum drug penetration through the skin, which was more than 50% at the end of 36 h. However, comparing OA release from OANPs (F3), the gel formulation (OAG1) exhibited more retard release behavior. This more sustained OA release from OAG1 is attributed to the prolonged skin contact time and enhanced hydration effect provided by the gel matrix, which facilitates better diffusion of OA across the stratum corneum. Upon hydration, electrostatic repulsion between the negatively charged carboxylic group of CP initiates expansion of molecules and turns the tightly packed interlocking structure into an uncoiled arrangement (Safitri *et al*., 2021; Chellam, 2025). This ultimately generates gel of appreciable strength with prominent adhesion. Moreover, sustained permeation could be facilitated by the gel's maximum viscosity due to viscoelastic and thixotropic polymers such as CP (Safitri *et al*., 2021; Ellakwa *et al*., 2024). As CP is reported to dissociate at basic pH, where it achieves maximum swelling and yields a thick viscous gel with appreciable gelling capacity due to the revelation of its carboxylic group (Moglad *et al*., 2020). Likewise, concomitant addition of HPMC along with CP further favored decreased permeation over time (Al-Zoubi *et al*., 2011). Additionally, the gel acts as a drug reservoir, allowing sustained release over time (Shakir *et al*., 2022; Sindhu *et al*., 2022b).

In contrast, the free OA suspension showed the least permeation at the application site. Though OANPs (F3) and free OA suspension may initially offer better penetration due to smaller particle size and increased surface area, they are more likely to detach quickly from the skin surface due to being less viscous, thereby reducing the bioadhesion or retention, contact time and ultimately the amount of drug permeated. The average drug retention (%) results presented in figure 6b revealed that the prepared gel formulation (OAG1) showed maximum retention (52.6%) compared to the free OA suspension and OANPs (F3). Conclusively, OAG1 demonstrated superior performance, possibly due to its optimized viscosity, polymeric blend composition and drug-polymer interactions, which may have contributed to promising drug release, permeation and retention.

CONCLUSION

The novelty of this study lies in developing an oleanolic acid nanoparticle-loaded topical gel to overcome the poor solubility, low dispersibility and limited topical availability of oleanolic acid. Nanonization improved surface area, dispersion and drug release, while incorporation into a gel enhanced topical application, skin residence time, local retention and sustained release. The comparison between optimized nanoparticles and the nanoparticle-loaded gel further demonstrated the contribution of the gel matrix to improved topical delivery, especially in the absence of a directly comparable commercial formulation.

The study successfully demonstrated the potential of OANPs prepared via nanoprecipitation as an effective drug delivery system. The nanoparticles exhibited excellent physical stability, retaining their structural integrity over extended storage durations. High drug entrapment efficiency confirmed that a substantial proportion of OA was successfully encapsulated, thereby enhancing the therapeutic payload and minimizing drug loss. The OANPs also exhibited notable biological activity, including strong antioxidant and antimicrobial effects. These findings suggest a dual therapeutic role for the nanoparticles, not

Article in Press

only as OA carriers but also as bioactive agents that contribute to overall therapeutic efficacy. *Ex-vivo* permeation studies further demonstrated the ability of OANPs to effectively deliver OA across the skin barrier. These results validate that the nanoparticle formulation facilitates both drug release and transdermal permeation, ensuring the active compound reaches underlying tissues where it can exert its therapeutic effect. Additionally, *in-vitro* drug release studies revealed a controlled and sustained release profile. This is a critical feature for modern drug delivery systems, as it enables the maintenance of steady therapeutic drug levels over time, reduces dosing frequency and enhances patient adherence to treatment regimens. Collectively, these findings highlight the promise of OANPs as a versatile and efficient platform for topical therapeutic applications.

Acknowledgment
The authors thankful to faculty of pharmacy, The University of Lahore, Pakistan for his valuable lab support throughout this work.

Authors' contributions
AN, MF, AH and HR: Conceptualized the study; AN, AH and HR: Contributed to manuscript writing and preparation; RS, NA, RK, SS, SA and HAI: Reviewed, edited and critically revised the manuscript. All authors read and approved the final version of the manuscript.

Funding
This work was supported by the Deanship of Scientific Research, Vice Presidency for Graduate Studies and Scientific Research, King Faisal University, Al-Ahsa, Saudi Arabia (Grant No. KFU261563).

Data availability statement
Data will be available from the corresponding author upon request.

Ethical approval
Ethical approval for this study was obtained from the Ethical Approval Committee, The University of Lahore, Pakistan, under approval numbers IREC-2025-3H and IREC-2025-3D. This study was performed in adherence with the ARRIVE guidelines. See supplementary file for the ARRIVE checklist.

Conflict of interest
The authors declare no conflict of interest.

REFERENCES

Abu-rumman A, Abu-huwaij R and Hamed R (2022). Development and *in-vitro* appraisal of Soluplus® and/or Carbopol® 971 buccoadhesive patches releasing atorvastatin. *J. Adhes.,* **98**(7): 915-933.

Ali MH, Azad MAK, Khan K, Rahman MO, Chakma U and Kumer A (2023). Analysis of crystallographic structures and properties of silver nanoparticles synthesized using PKL extract and nanoscale characterization techniques. *ACS omega.*, **8**(31): 28133-28142.

Alwan RM and Rajab NA (2021). Nanosuspensions of selexipag: Formulation, characterization and *in-vitro* evaluation. *Iraqi J. Pharm. Sci.*, **30**(1): 144-153.

Botha NL, Mushonga P and Onani MO (2023). Review on nanogels and their applications on dermal therapy. *Polym. Polym. Compos.*, **31(4)**: 0967311231192816.

Chellam NS (2025). Chemistry at the limit of space and time–from studies on aluminum nanocrystals to colloidal crystal engineering with DNA. *PhD diss*., Northwestern University.
https://www.proquest.com/openview/40a88766a4bcfa6cf3023a982ea0d1ad/1?pqorigsite=gscholar&cbl=18750&diss=y

De Stefani C, Lodovichi J, Albonetti L, Salvatici MC, Quintela JC, Bilia AR and Bergonzi MC (2022). Solubility and permeability enhancement of oleanolic acid by solid dispersion in poloxamers and γ-CD. *Mol.*, **27**(9): 3042.

Ellakwa TE, Abu-Khadra AS and Ellakwa DES (2024). Influence of physico-chemical properties of hydroxypropyl methylcellulose on quetiapine fumarate release from sustained release matrix tablets. *BMC chem.*, **18**(1): 219.

Farooq U, Rasul A, Sher M, Qadir MI, Nazir I, Mehmood Y, Riaz H, Shah PA, Jamil QA and Khan BA (2020). Development, characterization and evaluation of anti-fungal activity of miconazole based nanogel prepared from biodegradable polymer. *Pak. J. Pharm. Sci.*, **33**(1): 449-457.

Flieger J, Flieger W, Baj J and Maciejewski R (2021). Antioxidants: Classification, natural sources, activity/capacity measurements and usefulness for the synthesis of nanoparticles. *Mater.*, **14**(15): 4135.

Gulcin I and Alwasel SH (2023). DPPH radical scavenging assay. *Processes.*, **11**(8): 2248.

Iriventi P, Gupta NV, Osmani RAM and Balamuralidhara, V (2020). Design & development of nanosponge loaded topical gel of curcumin and caffeine mixture for augmented treatment of psoriasis. *DARU J. Pharm. Sci*., **28**(2): 489-506.

Jannus F, Sainz J and Reyes-Zurita FJ (2024). Principal bioactive properties of oleanolic acid, its derivatives and analogues. *Mol.*, **29**(14): 3291.

Jiamphun S and Chaiyana W (2023). Enhancing skin delivery and stability of vanillic and ferulic acids in aqueous enzymatically extracted glutinous rice husk by nanostructured lipid carriers. *Pharmaceutics.*, **15**(7): 1961.

Article in Press

Kaur J, Anwer MK, Sartaj A, Panda BP, Ali A, Zafar A, Kumar V, Gilani SJ, Kala C and Taleuzzaman M (2022). ZnO nanoparticles of Rubia cordifolia extract formulation developed and optimized with QbD application, considering *ex-vivo* skin permeation, antimicrobial and antioxidant properties. *Mol.*, **27**(4): 1450.

Kesharwani P, Jain A, Srivastava AK and Keshari MK (2020). Systematic development and characterization of curcumin-loaded nanogel for topical application. *Drug Dev. Ind. Pharm*., **46**(9): 1443-1457.

Khan AS, Shah KU, Mohaini MA, Alsalman AJ, Hawaj MAA, Alhashem YN, Ghazanfar S, Khan KA, Niazi ZR and Farid A (2022a). Tacrolimus-loaded solid lipid nanoparticle gel: Formulation development and *in-vitro* assessment for topical applications. *Gels*., **8**(2): 129.

Khan Y, Sadia H, Ali Shah SZ, Khan MN, Shah AA, Ullah N, Ullah MF, Bibi H, Bafakeeh OT and Khedher NB (2022b). Classification, synthetic and characterization approaches to nanoparticles and their applications in various fields of nanotechnology: A review. *Catalysts*., **12**(11): 1386.

Mahmood T, Sarfraz RM, Mahmood A, Salem-Bekhit MM, Ijaz H, Zaman M, Akram MR, Taha EI, Sahu RK and Benguerba Y (2024). Preparation, *in-vitro* characterization and evaluation of polymeric pH-responsive hydrogels for controlled drug release. *ACS omega*., 9(9): 10498-10516.

Moglad EH, Fatima F, Ahmed MM, Seshadri VD, Anwer MK and Aldawsari MF (2020). Development of topical antibacterial gel loaded with cefadroxil solid lipid nanoparticles: *In-vivo* wound healing activity and epithelialization study. *Int. J. Pharmacol*., **16**(4): 298-309.

Naz A, Farooq M, Sarfraz M, Unar A, Shakir R, Idrees HA and Anwar N (2026). Formulation and HPLC-UV−based quantification of nanoliposomes co-encapsulating genistein and oleanolic acid. *Int. J. Anal. Chem*., **1**: 6094234.

Naz A, Haider S, Khan MIU, Khokhar R, Rubab M, Farooq M, Afzal A and Sarfraz M (2025). *In-vitro* anticancer activity and biodistribution analysis of optimized hybrid nanoparticulate system co-loaded with apigenin and oleanolic acid. *J. Liposome Res*., **35**(4): 566-589.

Naz A, Haider S, Rana M, Malik N, Afzal A, Farooq M and Sarfraz M (2025). Quantification of oleanolic acid and apigenin in biological matrices following intraperitoneal administration of co-loaded nanoformulations: Method validation and biodistribution studies. *Talanta Open*., **11**: 100470.

Nikam AN, Roy A, Raychaudhuri R, Navti PD, Soman S, Kulkarni S, Shirur KS, Pandey A and Mutalik S (2024). Organogels: "Gel Volution" in topical drug delivery-present and beyond. *Curr. Pharm. Des*., **30**(7): 489-518.

Nnamani PO, Ugwu AA, Nnadi OH, Kenechukwu FC, Ofokansi KC, Attama AA and Lehr CM (2021). Formulation and evaluation of transdermal nanogel for delivery of artemether. *Drug Deliv. Transl. Res*., **11**(4): 1655-1674.

Pathak S, Sahu P, Begum JS, Kashaw SK, Pandey A, Semwal P and Sharma R (2024). Formulation and assessment of penetration potential of Risedronate chitosan nanoparticles loaded transdermal gel in the management of osteoporosis: *In-vitro* and *ex-vivo* screening. *Carbohydr. Polym. Technol. Appl*., **7**: 100440.

Patil N, Bhaskar R, Vyavhare V, Dhadge R, Khaire V and Patil Y (2021). Overview on methods of synthesis of nanoparticles. *Int. J. Curr. Pharm. Res*., **13**(2): 11-16.

Perry, D. L and Wren, A. W. 2026. Altering the pH during sol-gel synthesis of bioactive glass particles and its effect on structural and antibacterial properties. *J. Biomater. Appl*., **40**(8): 987-1002.

Pirtarighat S, Ghannadnia M and Baghshahi S (2019). Green synthesis of silver nanoparticles using the plant extract of Salvia spinosa grown *in-vitro* and their antibacterial activity assessment. *J. Nanostruct. Chem*., **9**(1): 1-9.

Rahim MA, Jan N, Khan S, Shah H, Madni A, Khan A, Jabar A, Khan S, Elhissi A and Hussain Z (2021). Recent advancements in stimuli responsive drug delivery platforms for active and passive cancer targeting. *Cancers*., **13**(4): 670.

Safitri FI, Nawangsari D and Febrina D (2021). Overview: Application of Carbopol 940 in gel. ICHMS (AHMS 2020). *Atlantis Press*., 80-84.

Shakir R, Hanif S, Salawi A, Arshad R, Sarfraz RM, Irfan M, Raza SA, Barkat K, Sabei FY and Almoshari Y (2022). Exorbitant drug loading of metformin and sitagliptin in mucoadhesive buccal tablet: *In-vitro* and *in-vivo* characterization in healthy volunteers. *Pharmaceuticals*, **15**(6): 686.

Shi Z, Pan S, Wang L and Li S (2021). Topical gel based nanoparticles for the controlled release of oleanolic acid: design and *in-vivo* characterization of a cubic liquid crystalline anti-inflammatory drug. *BMC Complement. Med. Ther*., **21**(1): 224.

Sindhu RK, Gupta R, Wadhera G and Kumar P (2022b). Modern herbal nanogels: Formulation, delivery methods and applications. *Gels*., **8**(2): 97.

Talele S, Nikam P, Ghosh B, Deore C, Jaybhave A and Jadhav A (2017). A research article on nanogel as topical promising drug delivery for diclofenac sodium. *Indian J. Pharm. Educ. Res*., **51 (4)**: S580-587.

Tang ZY, Li Y, Tang YT, Ma XD and Tang ZY (2022). Anticancer activity of oleanolic acid and its derivatives: Recent advances in evidence, target profiling and mechanisms of action. *Biomed. Pharmacother*., **145**: 112397.

Article in Press

Tetik G, Rencber S, Ozoglu ET, Yapar EA, Karavana SY and Ozer O (2021). Design and evaluation of topical antioxidant nanogel formulations. *J. Cosmet. Sci*., **72**(1): 47-62.

Wasim M and Bergonzi MC (2024). Unlocking the potential of oleanolic acid: Integrating pharmacological insights and advancements in delivery systems. *Pharmaceutics*., **16**(6): 692.

Yan L, Shen J, Wang J, Yang X, Dong S and Lu S (2020). Nanoparticle-based drug delivery system: A patient-friendly chemotherapy for oncology. *Dose-Response*., **18**(3): 1559325820936161.

Article in Press